Biomechanics and Modeling in Mechanobiology manuscript No.
(will be inserted by the editor)

Predicting isometric force from muscular activation using a physiologically inspired model

Heiko Wagner · Kim Boström · Bastian Rinke

December 21, 2010

Abstract Motivated by biochemical processes during muscular contraction, a model is constructed that predicts isometric force from surface electromyographic signals (sEMG). The model is experimentally validated and then it is used to predict contractions from sEMG data. The calculated simulations reveals a highly nonlinear relationship between sEMG and isometric force.

Keywords muscular model · surface EMG · isometric contraction · parameter estimation · model validation

1 Introduction

In a clinical setting as well as in the field of sports science, motor control, or robotics, non-invasive methods are necessary to investigate or improve the diagnosis of neurological and orthopedic condition in humans (Erdemir et al 2007). Therefore, several approaches to estimate the resultant joint torques and forces have been developed in the past (Buchanan et al 2004; Granata and Marras 1993; Hof and Van den Berg 1981; Jonkers et al 2002; Seth and Pandy 2007).

Usually, muscular forces are calculated by the external moments they produce. However, these moments are often the result of the contraction of many different muscles. To determine these loads based on musculoskeletal models, it is necessary to know the activation of the involved muscles during a specific movement (Koo and Mak 2005; Lloyd and Besier 2003; Manal and Buchanan 2003; Langenderfer et al 2005). A very common method to measure the muscular activation is the surface electromyography (sEMG). Between sEMG and muskular forces, both linear (Hof and van den Berg 1977; Lippold 1952) and non-linear (Lindström et al 1974; Vredenbregt and Rau 1973) relationships have been found. However, the proposed models are not physiologically motivated. Moreover, the sEMG signals are mostly heavily filtered which unavoidably results in a loss of information. Altogether, these models can only be regarded as relatively coarse heuristic approximations (Gottlieb and Agarwal 1971; McGill 1992).

A physiologically motivated model to describe the activation dynamics within a muscle is, to our knowledge, still lacking. However, there are already physiological Hill-type muscle models to describe the muscular force production (Thaller and Wagner 2004; Zajac 1989; Hill 1938). Based on these models we have developed a method to determine the model parameters of subjects individually with a nonlinear least square fitting method in a former study (Wagner et al 2005).

It is the aim of the present study to construct a physiologically inspired model which allows one to calculate isometric force from measured sEMG, and which is based on a low number of parameters, such that they can be determined experimentally for individual subjects. The validity of the model is in a first step verified by experimental test, and in a second step it is used to predict similar contractions from individually measured sEMGs. With our model, we hope to improve the understanding of the processes inside the muscle during isometric contraction. It may further be beneficial that the capability of predicting force from single muscle activation allows the prediction of more complex dynamic movements in a clinical setting.

Motion Science, Westfälische Wilhelms-University of Münster
& Center for Nonlinear Science (CeNoS)
Horstmarer Landweg 62b, 48149 Münster, Germany
E-mail: heiko.wagner@uni-muenster.de

2 Methods

2.1 Model

The model consists of two different levels that deal with the different stages of force production inside the muscle. The first level of the model describes the increase of Ca^{2+} concentration inside the sarcoplasm, while the second level describes the contraction and relaxation characteristics of the muscle at a given Ca^{2+} concentration. In the following we consider the Ca^{2+} concentration $C(t)$, the EMG activity $E(t)$, and the force production $F(t)$ each being normalized to their respective maximum. As a consequence, the units of all model parameters will be dimensionless.

First level: Development of Ca^{2+} concentration Initiated by the neural activation of the muscle, the membrane of the activated muscle cell gets permeable for Ca^{2+} ions, causing the Ca^{2+} concentration to rise instantly. In first approximation, the Ca^{2+} influx is thus proportional to the sEMG signal. The initial slope of concentration between sarcoplasmatic reticulum and sarcoplasm is falling with the duration of its permeability, so the influx gets smaller when the latter approaches its maximum at unity. Furthermore, the reflux of Ca^{2+} behaves complementarily to the influx. Hence summing up, the Ca^{2+} concentration $C(t)$ can be described by the differential equation

$$\dot{C}(t) = P_1 \cdot E(t) \cdot (1 - C(t)) - P_2 \cdot (1 - E(t)) \cdot C(t), \qquad (1)$$

where P_1 and P_2 are proportionality constants governing the rates of influx and reflux, respectively. On the plausible assumption that Ca^{2+} ions are flowing in and out of the sarcoplasm permanently, the sEMG signal reflects saturation properties of the sarcoplasmatic Ca^{2+} concentration. Realistically, the influx of Ca^{2+} ions to the sarcoplasm does not lead to instant contraction at each level of concentration, hence we introduce as another model parameter the threshold S below which no contractional processes are initiated, so that

$$C(t) := 0 \quad \text{for} \quad C(t) \leq S. \qquad (2)$$

Second level: Force production through muscular activation and relaxation Increased Ca^{2+} concentration is immediately followed by muscular contraction. However, reaching the final force level usually takes some time depending on the amplitude of the final force (Gottlieb and Agarwal 1971; Zajac 1989). These characteristics are described in the second level of the model. In first approximation, the muscular activation is proportional to the Ca^{2+} concentration in the sarcoplasm. Furthermore, the muscular activation should be smaller the closer the force gets to its maximum at unity. Lastly, the muscular relaxation should behave complementary to the muscular activation. Summing up, the total force production $F(t)$ of the muscle is described by the differential equation

$$\dot{F}(t) = P_3 \cdot C(t) \cdot (1 - F(t)) - P_4 \cdot F(t) \cdot (1 - C(t)), \qquad (3)$$

where P_3 and P_4 are proportionality constants governing the rates of muscular activation and relaxation, respectively (cf. Zajac (1989), eq. 6, p.374). The force measured in the experimental setup is not the force generated by the muscle but rather the force in the hand. If the assumptions hold true, the two forces are related through a constant gearing dependent on the geometry. For non-isometric measurements the gearing depends on the elbow angle and must then be included in the model.

The differential equations (1) and (3) are numerically solved using a Dormand-Prince-Solver implemented in MATLAB (The MathWorks, Version 2007a, Simulink Toolbox). Input to these equations are the measured sEMG data. To find individual sets of parameters for the subjects, the calculated model output F is first fitted to the externally measured force. The fitting procedure is done in MATLAB using a least-squares algorithm.

2.2 Experiment

Subjects Eleven healthy subjects (9 male, 2 female) were tested during this experiment with a mean age of 24.2 $\pm$ 1.75 years. All of them gave their informed consent during the experiment.

Exercise For validation of the constructed model, the exercise should involve as few muscles as possible because the sEMG signal of each individual muscle must be compared with its force which only can be measured externally. We chose an extension of the elbow joint as experimental exercise, a movement that is produced mainly by *m. triceps brachii* (*caput longum* and *laterale*), and marginally by *m. anconeus* and *m. triceps brachii* (*caput mediale*) (Putz and Pabst 2000). We used the activation of *m. triceps brachii* (*caput laterale*) as input for the model, since it was the best predictor for the externally measured force. Also the activation of the antagonist (*m. biceps brachii*) was recorded for to rate the scale of coactivation which potentially affects the externally measured force.

Data collection and experimental setup Activations of *m. triceps brachii* (*caput laterale*) and *m. biceps brachii* were recorded (electrode positions according to SENIAM) with bipolar surface electromyography (Biovision 5-700 Hz, AD conversion rate 2000 Hz, gain 2500, Superlogics, PCM12 Card: 12 bit, 16 channels). A force sensor (Biovision, measuring range 5 kN) was connected to a V-formed handhold

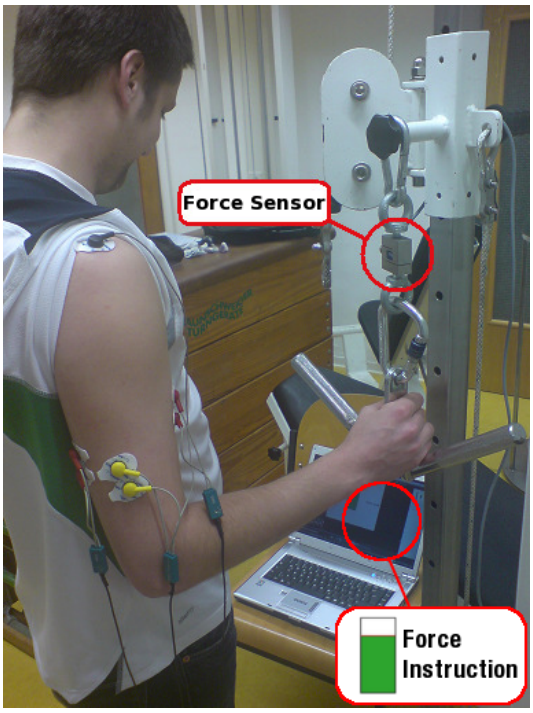

Fig. 1 Experimental setup. The subject applies the percentage of maximum force indicated by a bar on a computer display.

fixed on a pole at shoulder height of the subjects. The subjects stood in front of the construction with their right hands at the handhold. They were requested to take a particular body position while performing the contractions, such that isometric contraction was measured while the elbow joint was at an angle of 90 degrees. The subjects followed instructions displayed on a notebook in front of them, where a bar indicated the percentage of maximum force to be applied. No visual feedback of the actual force was given. Intervals of 21-25.5 s were measured, containing instructions to produce isometric contractions of 0, 25, 50, 75 or 100% of maximum voluntary contractions (MVC) for 1.5 or 3 s. Six sequences (A to F) with different chronology of contractions were presented to each subject. Sequence A was measured five times, sequences B to F one time (Table 1). Lastly, to determine the MVC level, the subjects were asked to perform maximum voluntary flexion and extension contractions.

Data analysis First, the mean value of muscular activation during the 0%-phases was subtracted from the entire sEMG signal to match the phases of neutral sEMG (background noise) to the phases of zero force production. Second, the sEMG data was filtered with a moving average filter (window width 5 ms) to reduce noise. Third, the filtered sEMG signal was normalized to its maximum. The same treatment was also applied to the measured force data. After these treatments both sEMG and force data were fed into the model.

Sequence	Applied force [%]	Duration [s]
A	0 50 0 25 75 0 100 0	8·3.0 = 24.0
B	0 75 0 50 0 100 25 0	8·3.0 = 24.0
C	0 25 50 0 75 100 0	7·3.0 = 21.0
D	0 50 75 0 25 100 0	7·3.0 = 21.0
E	0 25 0 50 0 25 0 50 0 75 0 100 0 75 0 100 0	17·1.5 = 25.5
F	0 25 50 75 100 0 0 75 0 75 0 75 0 75 0	15·1.5 = 22.5

Table 1 Sequences of force instructions to be applied by the subject. The force instructions are presented on a monitor in front of the subject.

For each subject, five independent measurements corresponding to sequence A were used to determine the individual sets of parameters. For each subject $s = 1,\ldots,11$ and each trial $r = 1,\ldots,5$, the algorithm yielded $i = 1,\ldots,4$ parameters $P_i = P_{ir}(s)$ and a threshold value $S = S_r(s)$, together with a value $\delta = \delta_r(s)$ for the goodness of fit between simulated and measured forces, which was quantified by the residual variance, that is, the sample-averaged squared Euklidean distance between data and model function,

$$\delta = \sqrt{\frac{1}{N}\sum_{n=1}^{N}(x_n - f_n)^2}, \tag{4}$$

where $N = f \cdot T$ is the number of samples with f being the measurement frequency and T being the measurement time, and where x_n are the data samples taken at respective times t_n, and where $f_n = f(t_n)$ are the corresponding model function values.

Next, the parameter sets $P_{ir}(s)$ and $S_r(s)$ were averaged over the trials $r = 1,\ldots,5$ to give the mean parameter sets $\overline{P}_i(s)$ and $\overline{S}(s)$. Based on these mean parameter sets, the forces during the sequences B to F were for each subject predicted by the model and compared to the experimentally measured forces using the distance measure δ. A two-way ANOVA was performed on the parameter sets $\overline{P}_i(s)$ with the parameter index i and the subject index s constituting the two factors, thereby making it possible to investigate inter-individual and intra-individual effects.

3 Results

3.1 Determination of model parameters

The results from the fitting procedure are shown in Table 2. A two-way ANOVA on the parameters $P_i(s)$, with the parameter index i and the subject index s as the two factors, shows that there is a highly significant inter- and intra-subjective variability ($p < 10^{-6}$ for both factors). This means that the model parameters $P_1,\ldots,P_4$ are not universal but

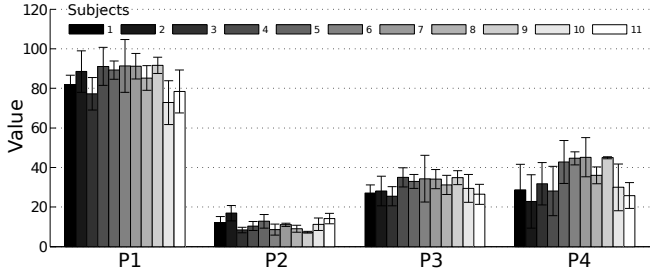

Fig. 2 Mean values and standard deviations of the model parameters $P_1,\ldots,P_4$ for each subject $1,\ldots,11$, determined by fitting the model to five independent datasets of sEMG data per subject, obtained on force sequence A (Table 1). The units of the parameters are dimensionless. The threshold parameter S is very small in comparison and is not shown here (cf. Table 2).

are adapted to each subject individually, and that the parameters are also significantly different for each subject individually. As can be seen from Figure 2, parameters P_1 and P_2 differ much more from each other than parameters P_3 and P_4. To find out whether P_3 and P_4 alone differ significantly from each other, we performed a corresponding posthoc test. A two-way ANOVA on the two parameter sets $P_{3r}(s)$ and $P_{4r}(s)$ with $r = 1,\ldots,5$ still reveals a significant intra-subjective difference ($p < 0.017$). However, when the trials are averaged to give the inter-subjective values $\overline{P}_3(s)$ and $\overline{P}_4(s)$, a paired t-test reveals no significant difference any more ($p \approx 0.08$). Hence though there can be assumed to be a significant intra-subjective difference between P_3 and P_4, this difference is rather subtle and may disappear under certain experimental circumstances, in particular when averaging individual trials per subject, or when performing only one trial per subject and measurement condition.

Subject	$\overline{P}_1$	$\overline{P}_2$	$\overline{P}_3$	$\overline{P}_4$	$\overline{S}$	$\overline{\delta}[\%]$
1	81.86	12.11	27.06	28.74	0.017	4.45
2	88.52	16.90	28.11	22.83	0.005	3.37
3	77.23	8.37	25.46	31.79	0.011	3.82
4	91.09	10.39	35.05	28.08	0.007	3.49
5	89.22	12.78	32.92	42.76	0.018	4.84
6	91.33	8.59	34.30	44.65	0.015	4.79
7	91.17	11.03	34.08	45.15	0.014	4.03
8	85.21	8.99	31.23	36.00	0.022	3.70
9	91.55	7.24	34.82	44.93	0.017	4.14
10	72.78	11.26	29.44	29.97	0.007	3.28
11	78.38	14.22	26.46	25.77	0.007	3.81
Total mean	85,30	11.08	30.81	34.61	0.013	3.97

Table 2 Mean parameter and goodness of fit values for each subject and their total mean, obtained from fitting the model to sEMG data corresponding to sequence A.

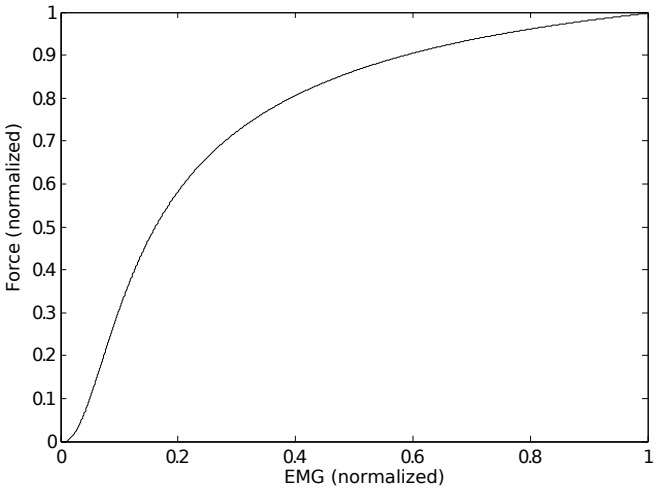

Fig. 5 Predicted relationship between sEMG and isometric force, estimated from averaging over all subjects.

Overall, the deviation δ of the simulated forces from the measured forces during the five trials of sequence A did not exceed 5%. Generally, the simulated forces showed an increased deviation at a high levels, certainly due to the increased variability of the measured forces at these levels (Figure 3, seconds 19-23).

3.2 Model predictions

After having determined a set of parameters for each subject from sequence A, these sets have been used to predict the contraction sequences B to F. Exemplarily, Figure 4 shows a simulated force curve analogously to Figure 3. Overall, the deviation δ of predicted forces from measured forces was only slightly larger than the deviation from reproduced forces from measured forces, and remained below 6 %.

Relationship between sEMG and generated force The relationship between sEMG-activity and isometric force production is calculated with a representative set of parameters $\overline{P}_i = \langle \overline{P}_i(s) \rangle$ averaged over all subjects. This relationship turns out highly non-linear, with an over-proportional increase of force at low activation levels, and an under-proportional increase of force at high activation levels (Figure 5).

Antagonistic coactivation The muscular coactivation of *m. biceps brachii* was shown to be only at 2-3% of maximal activation during the active phases of the exercise. Thus, it had negligible effect on the results of this study.

4 Discussion

Model validation Our results indicate that the simple physiological model considered here was able to faithfully re-

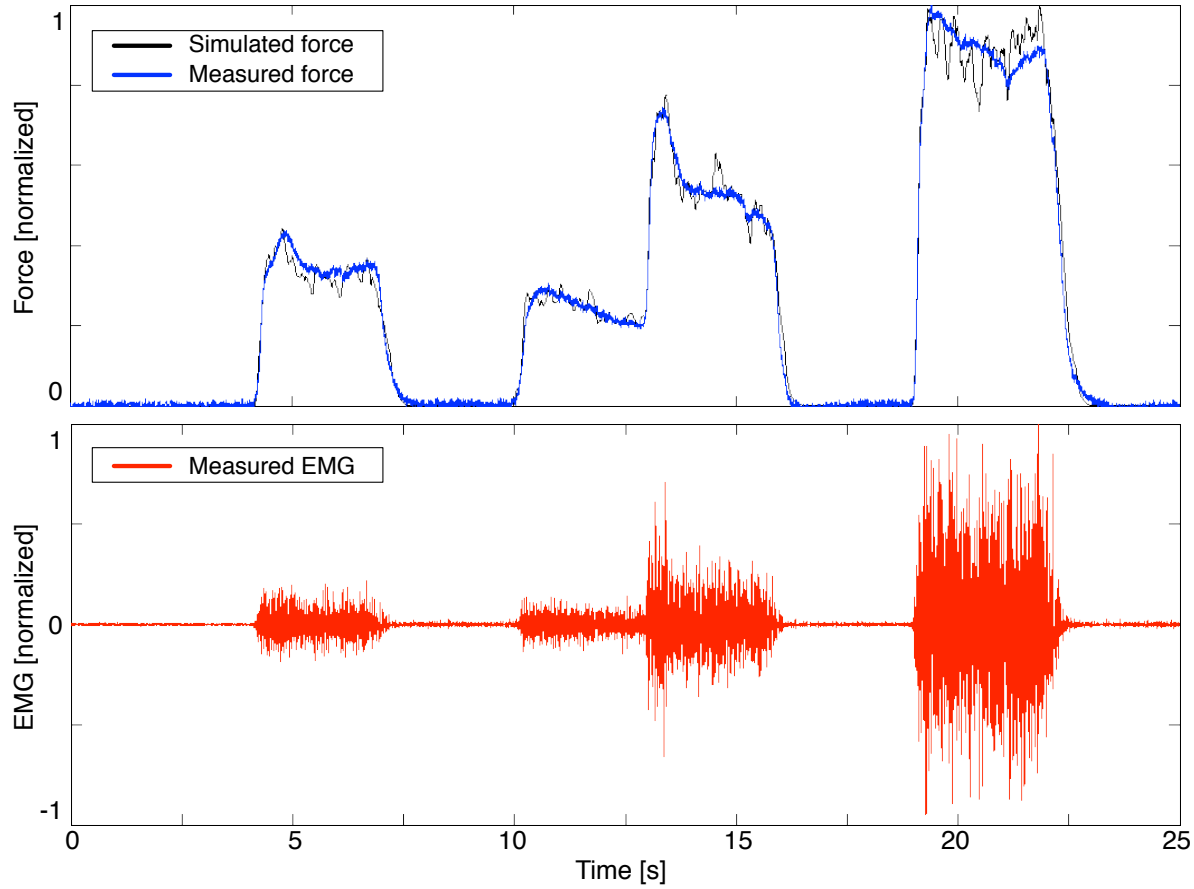

Fig. 3 Model fitting procedure, exemplarily shown for subject V10 on third run of sequence *A*. Top: Simulated (black) and measured force (blue); deviation is $\delta = 3.0\%$. Bottom: Corresponding EMG activity. Force and EMG data are normalized to their respective maximum.

produce and predict measured contractions. The distance δ between measured and simulated forces remains below 5% per sample. Such deviation is already small and mainly produced at higher force levels, which is not surprising considered that the subjects presumably did not apply their true maximum force in every trial. As a consequence, both sEMG and force signals would be normalized with underestimated values, accounting for higher deviations from the true value at higher levels of muscular activation, in agreement with the observations. Furthermore, the application of high force levels might result in a motion of the scapula and hence a reduced length of the triceps muscle. Additionally, at high force levels the serial elastic tendon element will be stretched, which also reduces the muscle length. A variation of muscle length affects the amount of muscular force production which in turn violates the isometric assumption. This effect is not included in our model and may be another reason for the stronger deviations between model data and experimental data at high force levels. Lastly, the overall precision of the force applied by the subjects might have been increased by giving a visual feedback of the actually measured force level. This additional precision would likely yield an even better match of the experimental data to the model. We thank the reviewer for making a respective suggestion to improve future experimental setups.

Physiological interpretation The model contains five parameters describing specific characteristics of the activation dynamics. The inter-individual distinguishability of the model parameters, that is, the ability of the model to significantly distinguish between subjects based on the model parameters, indicates that the parameters are not universal but rather subject specific. Parameter P_1 turns out to be much larger than P_2, which implies that the Ca^{2+} ions are flowing considerably faster into the sarcoplasm than they flow out. This matches the observation that the electromechanical delay is much shorter during contraction than during relaxation. The differences between P_3 and P_4 are rather subtle, although statistically significant, and may approximately be neglected. Physiologically this means that the muscular activation takes about the same time as the relaxation. If one neglects the subtle difference between P_3 and P_4 and combines the two parameters into one single parameter P_F, equation (3) simplifies to

$$\dot{F}(t) = P_F \cdot (C(t) - F(t)). \tag{5}$$

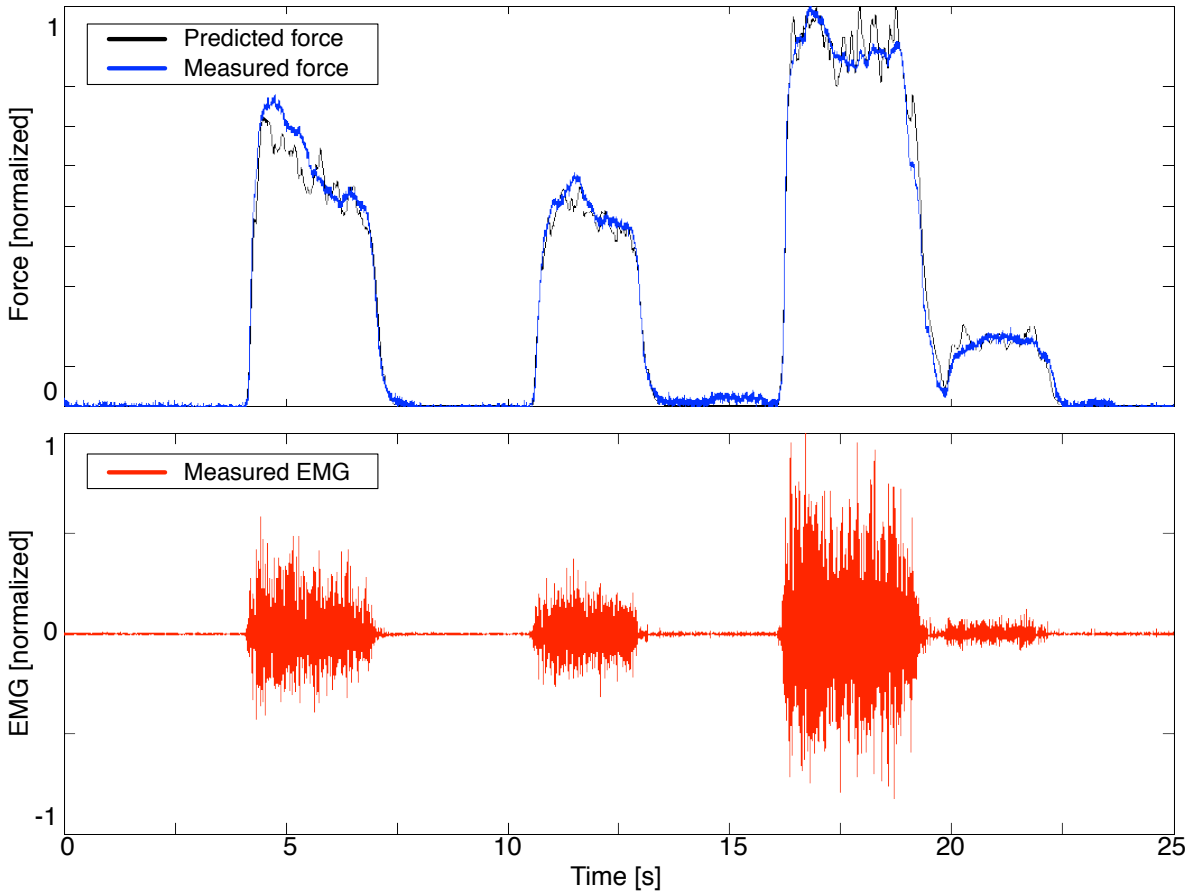

Fig. 4 Model prediction, exemplarily shown for subject V10 on third run of sequence *B*. Top: Predicted (black) and measured force (blue); deviation is $\delta = 3.3\%$. Bottom: Corresponding EMG activity. Force and EMG data are normalized to their respective maximum.

Interestingly, the above expression coincides with a widely accepted formula (Sust et al 1997), so our model might provide a physiological explanation for the latter.

Relationship between muscle activation and force The relationship between sEMG and force predicted by the model is highly non-linear (Figure 5). There is a strong effect of activation on force production at low levels, and a saturation effect at high levels. This result coincides qualitatively with other non-linear relationships found in the literature (Lindström et al 1974; Vredenbregt and Rau 1973).

Electromechanical delay In our model we neglected the mechanical factors involved in muscular contraction and relaxation, e.g. tendon elasticity. Therefore, simulated force production starts instantaneously with neuronal activation, although the maximum force is reached only at a certain time after neuronal activation has reached its maximum. Concerning the relaxation of the muscle after neuronal deactivation, simulations have been run during which the muscle got deactivated between 20 and 200 ms. The corresponding simulated force reached its saturation approximately after 400 ms, and by approx. 200 ms, 80% of force was annihilated. It is plausible to assume that mechanical factors here neglected will add up to the mere "electrochemical delay" here considered, to form the overall electromechanical delay well-known in experimental research (Vint et al 2001; Hopkins et al 2007; Muraoka et al 2004; Zhou et al 1995).

Applicability to other muscles For the validation of the model, the m. triceps brachii was chosen because it is a superficial muscle and one can assume a constant gearing between the muscle force and the externally measured force. This holds for other skeletal muscles as well, e.g. extensors and flexors at the knee joint and the ankle. If the musculoskeletal geometry becomes more complex, e.g. at the spinal column, then it should be adequately implemented in the model. Nonetheless, the relationship between muscular activation and force production should remain largely unaffected by these complications.

Limitations and potential improvements An obvious limitation of the model is its restriction to isometric muscle contractions. To overcome this limitation, the individual parameters of the model could be combined with individual

muscular parameters derived, for example, with the help of the ISOFIT method (Wagner et al 2005). Secondly, surface EMGs and externally measured forces generally capture the activity of several muscles simultaneously. Up to now, the direct measurement of an individual muscle still requires an invasive intervention. Thus while a model-based approach provides a possibility to avoid such invasive intervention, on the other hand for exactly the same reason the validation of the model remains limited. Lastly, an already mentioned limitation is the negligence of biomechanical factors like tendon length and elasticity. It is by now possible to non-invasively measure the movement of the tendon by ultrasound (Maganaris and Paul 2000; Mademli and Arampatzis 2008), so the missing factors could be included in the model and adapted to experimental data.

5 Summary

In the present study, a straightforward, physiologically motivated model for isometric contraction was introduced and validated. The model was able to accurately reproduce and predict muscle force from measured surface EMG data.

The method can be applied in physical therapy and sports sciences. An accompanying analysis of the sEMG based on our model may give some advice whether changes of external forces are due to a muscular hypertrophy or neuronal adaptations, for example in elderly people and chronic pain patients. In this context, the combination of our model with other already existing EMG driven models might be fruitful, in particular models that are used to quantify movements with respect to their effect on the stability of the trunk (Cholevicki and McGill 1996).

Altogether, in order to determine forces non-invasively and straightforwardly, the model-based approach promises to be a useful and adequate tool, e.g. in the field of physical therapy, sports science, and motor control.

6 Acknowledgements

We would like to thank Daniel Kohle for his valuable support during the preparation of the manuscript, and the reviewer for fruitful suggestions. The work of HW & KB were supported by the Federal Ministry of Education and Research (BMBF) [01EC1003A].

References

Buchanan TS, Lloyd DG, Manal K, Besier TF (2004) Neuromusculoskeletal modeling: estimation of muscle forces and joint moments and movements from measurements of neural command. J appl biomech 20(4):367–95

J Cholewicki and S M McGill (1996) Mechanical stability of the in vivo lumbar spine: implications for injury and chronic low back pain. Clin Biomech (Bristol, Avon), 11(1):1-15

Erdemir A, McLean S, Herzog W, van den Bogert AJ (2007) Model-based estimation of muscle forces exerted during movements. Clin Biomech (Bristol, Avon) 22(2):131–54

Gottlieb GL, Agarwal GC (1971) Dynamic relationship between isometric muscle tension and the electromyogram in man. J Appl Physiol 30(3):345–51

Granata KP, Marras WS (1993) An emg-assisted model of loads on the lumbar spine during asymmetric trunk extensions. J Biomech 26(12):1429–38.

Hill A (1938) The heat of shortening and the dynamic constants of muscle. ProcRoySoc (B) London 126:136–195

Hof AL, van den Berg J (1977) Linearity between the weighted sum of the emgs of the human triceps surae and the total torque. J Biomech 10(9):529–39

Hof AL, Van den Berg J (1981) Emg to force processing ii: Estimation of parameters of the hill muscle model for the human triceps surae by means of a calfergometer. J Biomech 14(11):759–70

Hopkins JT, Feland JB, Hunter I (2007) A comparison of voluntary and involuntary measures of electromechanical delay. Int J Neurosci 117(5):597–604

Jonkers I, Spaepen A, Papaioannou G, Stewart C (2002) An emg-based, muscle driven forward simulation of single support phase of gait. J Biomech 35(5):609–19

Koo TK, Mak AF (2005) Feasibility of using emg driven neuromusculoskeletal model for prediction of dynamic movement of the elbow. J Electromyogr Kinesiol 15(1):12–26

Langenderfer J, LaScalza S, Mell A, Carpenter JE, Kuhn JE, Hughes RE (2005) An emg-driven model of the upper extremity and estimation of long head biceps force. Comput Biol Med 35(1):25–39

Lindström L, Magnusson R, Petersen I (1974) Muscle load influence on myoelectric signal characteristics. Scand J Rehab Med Suppl 3:27 – 148

Lippold OCJ (1952) The relation between integrated action potentials in a human muscle and its isometric tension. J Physiol 117(4):492–9

Lloyd DG, Besier TF (2003) An emg-driven musculoskeletal model to estimate muscle forces and knee joint moments in vivo. J Biomech 36(6):765–76

Lida Mademli and Adamantios Arampatzis (2008). Mechanical and morphological properties of the triceps surae muscle-tendon unit in old and young adults and their interaction with a submaximal fatiguing contraction. J Electromyogr Kinesiol, 18(1):89-98

Maganaris, CN and Paul, JP (2000). Load-elongation characteristics of in vivo human tendon and aponeurosis. J Exp Biol, 203(Pt 4):751-6.

Manal K, Buchanan TS (2003) A one-parameter neural activation to muscle activation model: estimating isometric joint moments from electromyograms. J Biomech 36(8):1197–202

McGill SM (1992) A myoelectrically based dynamic three-dimensional model to predict loads on lumbar spine tissues during lateral bending. J Biomech 25(4):395–414

Muraoka T, Muramatsu T, Fukunaga T, Kanehisa H (2004) Influence of tendon slack on electromechanical delay in the human medial gastrocnemius in vivo. J Appl Physiol 96(2):540–4

Putz R, Pabst R (2000) Sobotta – Atlas der Anatomie des Menschen, vol 1 Kopf, Hals, obere Extremität. Urban & Fischer: München, Jena

Seth A, Pandy MG (2007) A neuromusculoskeletal tracking method for estimating individual muscle forces in human movement. J Biomech 40(2):356–66

Sust M, Schmalz T, Beyer L, Rost R, Hansen E, Weiss T (1997) Assessment of isometric contractions performed with maximal subjective effort: corresponding results for eeg changes and force measure-

ments. Int J Neurosci 92(1-2):103–18.
Thaller S, Wagner H (2004) The relation between hill's equation and individual muscle properties. J Theor Biol 231(3):319–32
Vint PF, McLean SP, Harron GM (2001) Electromechanical delay in isometric actions initiated from nonresting levels. Med Sci Sports Exerc 33(6):978–83
Vredenbregt J, Rau G (1973) Surface electromyography in relation to force, muscle length and endurance. New Developments in EMG and Clinical Neurophysiology pp 607 – 622
Wagner H, Siebert T, Ellerby DJ, Marsh RL, Blickhan R (2005) Isofit: a model-based method to measure muscle-tendon properties simultaneously. Biomech Model Mechanobiol 4(1):10–9
Zajac F (1989) Muscle and tendon: properties, models, scaling, and application to biomechanics and motor control. CritRevBiomedEng 17(4):359–411
Zhou S, Lawson DL, Morrison WE, Fairweather I (1995) Electromechanical delay in isometric muscle contractions evoked by voluntary, reflex and electrical stimulation. Eur J Appl Physiol Occup Physiol 70(2):138–45